









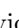

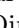






Kauffman Model with Spatially Separated Ligation and Cleavage Reactions

Johannes Josef Schneider^{1,2} , Peter Eggenberger Hotz¹,
William David Jamieson³ , Alessia Faggian⁴ , Jin Li² ,
Hans-Georg Matuttis⁵, Adriano Caliarì⁴ , Mathias Sebastian Weyland¹ ,
Dandolo Flumini¹ , Aitor Patiño Diaz⁴ , Silvia Holler⁴ ,
Federica Casiraghi⁴ , Lorena Cebolla Sanahuja⁴,
Martin Michael Hanczyc^{4,6} , David Anthony Barrow² ,
Pantelitsa Dimitriou² , Oliver Castell³ , and Rudolf Marcel Fuchsli^{1,7} 

¹ Institute of Applied Mathematics and Physics, School of Engineering, Zurich University of Applied Sciences, Technikumstr. 9, 8401 Winterthur, Switzerland
johannesjosefschneider@googlemail.com, {scnj,egg,weyl,flum,furu}@zhaw.ch

² School of Engineering, Cardiff University, Queen's Buildings, 14-17 The Parade, Cardiff, Wales CF24 3AA, UK

{LiJ40,Barrow,dimitriou}@cardiff.ac.uk

³ Welsh School of Pharmacy and Pharmaceutical Science, Cardiff University, Redwood Building, King Edward VII Ave, Cardiff, Wales CF10 3NB, UK

{jamieson,Castell10}@cardiff.ac.uk

⁴ Laboratory for Artificial Biology, Department of Cellular, Computational and Integrative Biology (CIBIO), University of Trento, 38123 Trento, Italy
{alessia.faggian,adriano.caliari,aitor.patino,silvia.holler,federica.casiraghi,lorena.cebolla,martin.hanczyc}@unitn.it

⁵ Department of Mechanical Engineering and Intelligent Systems, The University of Electrocommunications, Chofu Chofugaoka 1-5-1, Tokyo 182-8585, Japan
hg@mce.uec.ac.jp

⁶ Chemical and Biological Engineering, University of New Mexico, MSC01 1120, Albuquerque, NM 87131-0001, USA

⁷ European Centre for Living Technology, Ca' Bottacin, Dorsoduro 3911, 30123 Venice, Italy

<https://www.zhaw.ch/en/about-us/person/scnj/>

Abstract. One of the open questions regarding the origin of life is the problem how macromolecules could be created. One possible answer is the existence of autocatalytic sets in which some macromolecules mutually catalyze each other's formation. This mechanism is theoretically described in the Kauffman model. We introduce and simulate an extension of the Kauffman model, in which ligation and cleavage reactions are spatially separated in different containers connected by diffusion, and provide computational results for instances with and without autocatalytic sets, focusing on the time evolution of the densities of the vari-

This work has been partially financially supported by the European Horizon 2020 project *ACDC – Artificial Cells with Distributed Cores to Decipher Protein Function* under project number 824060.

© The Author(s) 2024

M. Villani et al. (Eds.): WIVACE 2023, CCIS 1977, pp. 141–160, 2024.

https://doi.org/10.1007/978-3-031-57430-6_12

ous molecules. Furthermore, we study the rich behavior of a randomly generated instance containing an autocatalytic metabolism, in which molecules are created by ligation processes and destroyed by cleavage processes and vice versa or generated and destroyed both by ligation processes.

Keywords: Kauffman model · origin of life · chemical evolution · Fick diffusion · autocatalytic set

1 Introduction

Over the past decades, the Kauffman model [11–13] has been intensively studied [7, 9, 10, 21]. It deals with one of the basic questions of the origin of life [14] how macromolecules could be created via chemical evolution. As a possible answer, it proposes the emergence of autocatalytic sets in which some molecules are able to mutually catalyze each other’s formation and which are self-sustaining if some food source in the form of monomers or small oligomers is provided. The basic condition for the production of macromolecules from an autocatalytic set is that the framework of catalyzed ligation and cleavage reactions forms a graph which in principle allows the production of the desired macromolecules [8]. This condition is necessary but not sufficient. Also the dynamics has to be considered as e.g. in the work of Bagley and Farmer [1]: They define an autocatalytic metabolism (ACM) as a coupled set of catalyzed reactions which lead to permanent concentrations $p_i(t)$ for the various molecules i that significantly depart from values one would obtain without catalysis. Füchslin et al. [5] simulated the Kauffman model in one container: They chose appropriate values for the occurrence of catalyzed cleavage and ligation reactions, started off with $p_i(t = 0) = 1$ for all molecules, allowed only an inflow of two constituent monomeric molecules, and measured probabilities for the occurrence of an ACM and the sizes of the ACM by having a look at the final values of p_i for the non-monomeric molecules. If at least one of them was larger than a proposed threshold, an ACM existed in their system.

In nature, one will find that catalyzed reactions are often only performed under some specific conditions, as e.g. enzymes only work in specific pH ranges. We assume that these specific conditions which change spatially might increase the probability for the existence of autocatalytic sets leading to macromolecules required for more complex forms of life. In order to make a first step in investigating this assumption, we extend the work by Füchslin et al. [5] to a system comprised of two containers: In one container, only catalyzed cleavage reactions shall be performed, in the other container, only catalyzed ligation reactions. Both containers are connected, such that molecules can diffuse into the other container depending on the concentration difference and the diffusion constant. This paper is organized as follows: We describe in general our extended model with spatially separated ligation and cleavage reactions in Sect. 2 and provide the simulation details for its application to a system of copolymers in Sect. 3.

Computational results for two randomly generated instances, one of them containing an ACM and the other displaying no ACM, are discussed in Sect. 4, before a conclusion and an outlook to future work is given in Sect. 5.

2 Extension of the Kauffmann Model

Based on the statements above, we now extend the model to a system with multiple containers. We thus deal with unnormalized densities $p_{i,j}$ annotated with two indices, where the first index i denotes as before the number of the corresponding molecule and the new second index j denotes the number of the container. The time evolution of $p_{i,j}$ is described by a set of differential equations. The total derivative $dp_{i,j}/dt$ subsumes the various temporal changes of $p_{i,j}(t)$ imposed by different processes.

2.1 “In-Out” Processes

As most basic processes, we assume a constant inflow $k_{i,j,\text{in}}$ and an outflow which depends linearly on the density $p_{i,j}$ with a factor $k_{i,j,\text{out}}$ in each container:

$$\left(\frac{dp_{i,j}}{dt}\right)_{\text{in-out}} = k_{i,j,\text{in}} - k_{i,j,\text{out}} \times p_{i,j} \quad (1)$$

For these “in-out” processes, we consider the system of various containers as homogeneous, i.e., we set the k -parameters to the same values for all containers. Furthermore, we set all outflow-parameters for the various molecules to the same value. Second, we want to have the same amount of inflow for two constituting molecules with indices $i = 1$ and $i = 2$ only, all other molecules shall be created through ligation and cleavage processes. Thus, we have

$$k_{i,j,\text{out}} \equiv k_{\text{out}} > 0 \text{ and } k_{i,j,\text{in}} \equiv k_{i,\text{in}} = \begin{cases} k_{\text{in}} > 0 & \text{for } i = 1, 2 \\ 0 & \text{otherwise} \end{cases} . \quad (2)$$

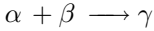
In the absence of other processes, these in-out processes would converge to an equilibrium in which

$$(p_{i,j})_{\text{in-out-equ}} = \begin{cases} \frac{k_{\text{in}}}{k_{\text{out}}} & \text{for } i = 1, 2 \\ 0 & \text{otherwise} \end{cases} \quad (3)$$

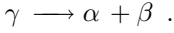
in all containers, to which also systems with reactions but no ACM converge.

2.2 Cleavage and Ligation Processes

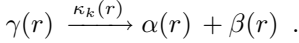
A ligation process is simply given by



and the corresponding cleavage process by



As already mentioned above, reactions enabled by catalyst molecules are considered within the Kauffman model. Let \mathcal{R} be the set of possible reactions and $R = |\mathcal{R}|$ be their number. Then, for cleavage reaction r , there is a set $\mathcal{K}(r)$ containing $K(r) = |\mathcal{K}(r)|$ catalyst molecules $\kappa_k(r)$, $k = 1, \dots, K(r)$, each of which is able to catalyze the reaction



Thus, for the cleavage reactions, we get the addend

$$\left(\frac{dp_{i,j}}{dt} \right)_{\text{cleavage}} = k_{j,C} \times \sum_{r=1}^R p_{\gamma(r),j} (-\delta_{i,\gamma(r)} + \delta_{i,\alpha(r)} + \delta_{i,\beta(r)}) \times \sum_{k=1}^{K(r)} p_{\kappa_k(r),j} \quad (4)$$

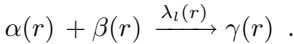
with the Kronecker symbol

$$\delta_{i,x} = \begin{cases} 1 & \text{if } i = x \\ 0 & \text{otherwise} \end{cases} \quad (5)$$

and the cleavage parameters $k_{j,C}$ relating the cleavage processes to the in-out processes.

Note that in the special case that there are no catalyst molecules for some cleavage reaction \tilde{r} , such that the reaction cannot be performed, the set of catalyst molecules is empty, $K(\tilde{r}) = 0$, and $\sum_{k=1}^0 \dots = 0$, such that this reaction does not contribute to the derivatives of the densities.

Analogously to the cleavage reactions, for each ligation reaction r , there is a set $\mathcal{L}(r)$ containing $L(r) = |\mathcal{L}(r)|$ catalyst molecules $\lambda_l(r)$, $l = 1, \dots, L(r)$, each of which is able to catalyze the reaction



Thus, for the ligation reactions, we get the addend

$$\left(\frac{dp_{i,j}}{dt} \right)_{\text{ligation}} = \sum_{r=1}^R k_{\alpha(r),\beta(r),j,L} \times p_{\alpha(r),j} \times p_{\beta(r),j} (\delta_{i,\gamma(r)} - \delta_{i,\alpha(r)} - \delta_{i,\beta(r)}) \times \sum_{l=1}^{L(r)} p_{\lambda_l(r),j} \quad (6)$$

with the ligation parameters $k_{\alpha(r),\beta(r),j,L}$. The reason behind making the ligation parameters depending on the molecules is the insight that if two different molecules get into close enough contact for a reaction, their corresponding end monomers must get into contact. For simplicity, we define

$$k_{\alpha,\beta,j,L} = \frac{k_{j,L}}{\Lambda(\alpha) \times \Lambda(\beta)} \quad (7)$$

with constant ligation parameters $k_{j,L}$ and $\Lambda(\alpha)$ and $\Lambda(\beta)$ being the lengths of molecules α and β , resp., which we define as the numbers of monomers in the molecules.

The dependency of the cleavage and ligation parameters $k_{j,C}$ and $k_{j,L}$ on the index j of the container allows us to separate cleavage and ligation processes spatially as intended:

- If we intend to have only cleavage processes in some specific container \hat{j} , then we set $k_{\hat{j},L} = 0$ and $k_{\hat{j},C}$ to some non-vanishing value.
- Analogously, if we intend to have only ligation processes in some specific container \tilde{j} , then we set $k_{\tilde{j},C} = 0$ and $k_{\tilde{j},L}$ to some non-vanishing value.

2.3 Consideration of Finite Energy Amounts

In [5], the authors extend the Kauffman model by introducing an energy consideration: For many cleavage and ligation reactions in nature, an activation energy is required. However, the available amount of energy is rather limited. So far, the formulas (4) and (6) assume an infinite amount of energy or at least a large and renewable amount of energy which provides no obstacle for the reactions to be executed.

In order to include energy restrictions, a further variable ε_j is introduced for each container j , with $\varepsilon_j(t)$ denoting the amount of energy available at time t in container j . In order to consider the energy, the right sides of Eqs. (4) and (6) need to be multiplied with ε_j and a further differential equation has to be added,

$$\begin{aligned}
 \left(\frac{d\varepsilon_j}{dt} \right)_{\text{total}} &= k_{E,j} - k_{E,j,\text{out}} \times \varepsilon_j \\
 &- \varepsilon_j \times k_{j,C} \times \sum_{r=1}^R p_{\gamma(r),j} \times \sum_{k=1}^{K(r)} p_{\kappa_k(r),j} \\
 &- \varepsilon_j \times \sum_{r=1}^R \frac{k_{j,L}}{\Lambda(\alpha(r)) \times \Lambda(\beta(r))} \times p_{\alpha(r),j} \times p_{\beta(r),j} \times \sum_{l=1}^{L(r)} p_{\lambda_l(r),j}
 \end{aligned} \tag{8}$$

with the energy inflow $k_{E,j}$, which we choose identical for all containers, i.e., then $k_{E,j} \equiv k_E$, and the outflow rate $k_{E,j,\text{out}}$, which we set identical with the corresponding parameter for all molecules, i.e., $k_{E,j,\text{out}} \equiv k_{\text{out}}$.

2.4 Diffusion Processes

So far, we only considered processes taking place separately in each container, such that we only have a set of separate containers up to now. But now, we want to take diffusion between neighboring containers into account. For simplicity, we

want to rely hereby on Fick's first law of diffusion [4], according to which the diffusion velocity v_D is given by

$$v_D = k_D \frac{\Delta c \times T}{\Delta x \times r \times \eta}, \quad (9)$$

with some diffusion constant k_D , the concentration difference Δc , the temperature T , the path length Δx which needs to be transversed, the radius r of the particle, and the viscosity η of the medium. In our case, the radius corresponds to the length $\Lambda(i)$ of molecule i and the concentration difference corresponds to the difference $p_{i,j} - p_{i,n}$ of the densities of molecule i in neighboring containers j and n . As diffusion processes occur only between neighboring pairs of containers, we need to create neighborhood lists: let $\mathcal{N}(j)$ be the set containing $N(j) = |\mathcal{N}(j)|$ index numbers of containers being neighbor to container j . Then we can write the addend for the diffusion processes as

$$\left(\frac{dp_{i,j}}{dt} \right)_{\text{diffusion}} = \sum_{n \in \mathcal{N}(j)} k_D \frac{p_{i,n} - p_{i,j}}{\Lambda(i)} = \frac{k_D}{\Lambda(i)} \times \left(-N(j)p_{i,j} + \sum_{n \in \mathcal{N}(j)} p_{i,n} \right) \quad (10)$$

with the diffusion constant k_D . As in Fick's first law of diffusion, the diffusion is proportional to the difference of the densities and inverse proportional to the length of the corresponding molecule. For containers of equal shape and volume with the same distance to all of their neighbors, we can omit the dependency on the path length.

Please note that we consider here only passive diffusion, i.e., diffusion does not use up any energy. Furthermore, only molecules can move to neighboring droplets, but there is no diffusion of energy in our model.

Such an approach with a time-independent diffusion constant k_D is at odds with the experimental reality: Experiments performed on the development of aHL pores opening channels in bilayers between droplets by William David Jamieson at Cardiff University clearly show that it takes a significant amount of time until the first pore is formed. Thereafter, the number of pores increases monotonously in time, with decreasing slope. Thus, we have to alter Eq. (10) in order to consider the increase of the number $m_{j,n}(t)$ of pores between the neighboring containers j and n :

$$\left(\frac{dp_{i,j}}{dt} \right)_{\text{diff.incr.}} = \frac{k_D}{\Lambda(i)} \sum_{n \in \mathcal{N}(j)} m_{j,n}(t) \times (p_{i,n} - p_{i,j}) \quad (11)$$

As the pores themselves are created by ligation of polymers (for example, aHL pores are comprised of seven macromolecules), one might think of considering the energy required for the creation of the pores, but we will abstain here from such an approach and neglect the energy consumption for the creation of pores. Furthermore, in order to show more clearly the effect of the opening of an increasing number of pores, we omit the dependencies of $m_{j,n}(t)$ on the container numbers j and n , i.e. $m_{j,n}(t) \equiv m(t)$.

3 Simulation Details

In this paper, we apply the Kauffman model to a set of reactions generating and splitting copolymers comprised of a linear sequence of two different monomers A and B. Thus, there are 2^A different molecules containing A monomers. (Please note that we assume the molecules to be directed, e.g. the molecules A – B and B – A are different molecules.) We consider only polymers comprised of up to a maximum number A_{\max} of monomers.

The total number M of different molecule types is given by

$$M = \sum_{A=1}^{A_{\max}} 2^A = 2^{A_{\max}+1} - 2. \quad (12)$$

The number R of cleavage reactions can be determined to

$$R = \sum_{A=2}^{A_{\max}} (A-1)2^A = A_{\max}2^{A_{\max}+1} - 2M. \quad (13)$$

In contrast to [5], we do not allow ligation reactions leading to molecules with more than A_{\max} monomers, such that the number of ligation reactions equals the number of cleavage reactions.

In our simulations, we use $A_{\max} = 3$, such that we have 12 non-monomeric different molecule types in our system and a reaction framework containing 20 possible reactions. For the various parameters, we choose values already used in [5]: The two monomers are not allowed to serve as catalysts, each of the other molecules is chosen with probability $r_C = 0.05$ to serve as catalyst for a cleavage reaction and with probability $r_L = 0.1$ to serve as catalyst for a ligation reaction. The other parameters are set to

$$k_{i,\text{in}} = \begin{cases} 1 & \text{for the monomers, i.e., for } i = 1, 2 \\ 0 & \text{otherwise} \end{cases},$$

$k_{\text{out}} = 0.02$, $k_C = 1$, $k_L = 1$, $k_E = 1$, and $k_D = 0.05$.

We will first have a look at the original Kauffman system with only one container for which we set $k_C = 1$ and $k_L = 1$. In order to study the effect of spatial separation of cleavage and ligation processes without any further side-effects occurring in more complex systems, we consider the extended Kauffman system with two containers only, one container $j = 1$, in which only cleavage reactions take place, and a second container $j = 2$, in which only ligation reactions are performed. For this purpose, we set $k_{1,C} = k_{2,L} = 1$ and $k_{1,L} = k_{2,C} = 0$.

We will also consider both diffusion processes as given in Eqs. (10) and (11). For the function $m(t)$, we choose

$$m(t) = \begin{cases} 0 & \text{if } t < 1 \\ \lfloor \log(t) \rfloor & \text{otherwise} \end{cases}. \quad (14)$$

This simple function is still able to reflect the key properties of the time evolution of the number of pores as observed in the experiment, i.e., the significant amount of time before the first pore opens up, the monotonous increase, and the concave shape after the opening of the first pore. As the pores open up at the times $t = e, e^2, e^3, \dots$ according to Eq. (14), the changes due to the opening of more pores are equally spaced out on a logarithmic time scale.

We use the Dormand-Prince method [3] for the numeric solution of the set of differential equations. This algorithm which belongs to the class of Runge-Kutta methods allows us to adaptively change the length of the time interval between successive time steps by determining two different solutions of fourth and fifth order and halving the length of the time interval if the deviation between them is too large. We redo the calculation with a halved time interval if the relative deviation exceeds a value of 10^{-8} . We integrate over the time interval from $t = 0$ to $t = 10^4$. As initial conditions, we set $p_{i,j}(t = 0) = \varepsilon_j(t = 0) = 1$ as in [5].

4 Computational Results

4.1 Revisiting the Original Kauffman Model Within One Container Only

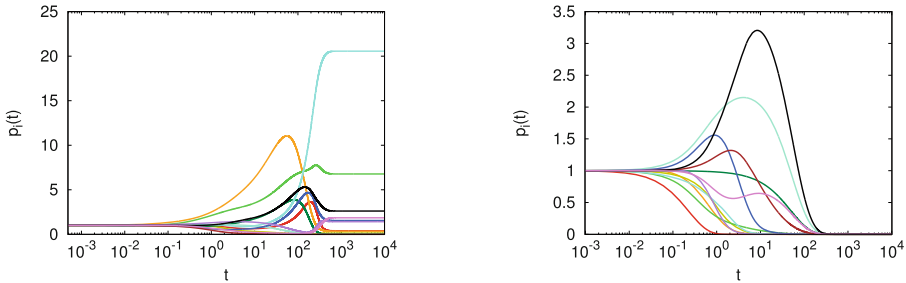


Fig. 1. Time evolution of the densities p_i of the non-monomeric molecules in the original Kauffman model with one container and without energy consideration, for a randomly created instance displaying an ACM (left) and another randomly created instance displaying no ACM (right)

We start out simulating the original Kauffman model in one container only and present results for two randomly created catalyzed reaction instances, one of them displaying an ACM and another one displaying no ACM. For the instance displaying an ACM, we provide the list of reactions in Table 1. We will use these two instances with the same random choice of catalyst molecules for the various reactions also in the simulations for the next scenarios and will use the same colors for the same molecules. The time evolutions of the densities $p_i(t)$ of all 12 non-monomeric molecules are shown for both instances in Fig. 1. In order to better

Table 1. List of reactions in the instance containing an ACM: In this instance, we have 14 successively numbered molecules, with the monomers being denoted as Nos. 1 and 2, and 20 possible reactions. In the right two columns, only those cleavage and ligation reactions are noted for which there is at least one catalyst molecule. This instance was randomly generated.

Reaction No.	reaction	cleavage	ligation
1	$3 \longleftrightarrow 1 + 1$		$1 + 1 \xrightarrow{5} 3$
2	$4 \longleftrightarrow 1 + 2$		$1 + 2 \xrightarrow{3,6,10,11,12,14} 4$
3	$5 \longleftrightarrow 2 + 1$		$2 + 1 \xrightarrow{4,6,8,12} 5$
4	$6 \longleftrightarrow 2 + 2$		
5	$7 \longleftrightarrow 1 + 3$		$1 + 3 \xrightarrow{4,12} 7$
6	$7 \longleftrightarrow 3 + 1$	$7 \xrightarrow{10} 3 + 1$	
7	$8 \longleftrightarrow 1 + 4$		
8	$8 \longleftrightarrow 3 + 2$		$3 + 2 \xrightarrow{12} 8$
9	$9 \longleftrightarrow 1 + 5$		$1 + 5 \xrightarrow{6} 9$
10	$9 \longleftrightarrow 4 + 1$	$9 \xrightarrow{8} 4 + 1$	$4 + 1 \xrightarrow{12,14} 9$
11	$10 \longleftrightarrow 1 + 6$	$10 \xrightarrow{5} 1 + 6$	
12	$10 \longleftrightarrow 4 + 2$		$4 + 2 \xrightarrow{5,9} 10$
13	$11 \longleftrightarrow 2 + 3$		$2 + 3 \xrightarrow{5,12,14} 11$
14	$11 \longleftrightarrow 5 + 1$		
15	$12 \longleftrightarrow 2 + 4$	$12 \xrightarrow{9} 2 + 4$	
16	$12 \longleftrightarrow 5 + 2$		$5 + 2 \xrightarrow{4} 12$
17	$13 \longleftrightarrow 2 + 5$		$2 + 5 \xrightarrow{7} 13$
18	$13 \longleftrightarrow 6 + 1$	$13 \xrightarrow{13} 6 + 1$	$6 + 1 \xrightarrow{11,13} 13$
19	$14 \longleftrightarrow 2 + 6$	$14 \xrightarrow{13} 2 + 6$	$2 + 6 \xrightarrow{7,8} 14$
20	$14 \longleftrightarrow 6 + 2$		$6 + 2 \xrightarrow{9} 14$

display the developments at short time scales, we use a logarithmic time scale. After some intermediate increases and decreases of the various densities, the system converges to final values for the various densities between $t = 5 \times 10^2$ and $t = 10^3$. The non-vanishing final values for some densities in the left picture indicate that this instance displays an ACM, whereas the finally vanishing densities in the right picture show that the second instance does not contain an ACM. For the instance with an ACM, the Dormand-Prince method needs 194059 time steps, whereas only 1772 are needed for the instance without an ACM. In order to get results of equal quality for the time evolution of the densities, much more computing time is needed for an instance with an ACM.

Please note that each color in the curves in Fig. 1 corresponds to one distinct molecule. We will use the same color for the same distinct molecule in the curves of Figs. 2, 3, 4, 5, 6, 7 and 8 and in the boxes in Figs. 9, 10 and 11.

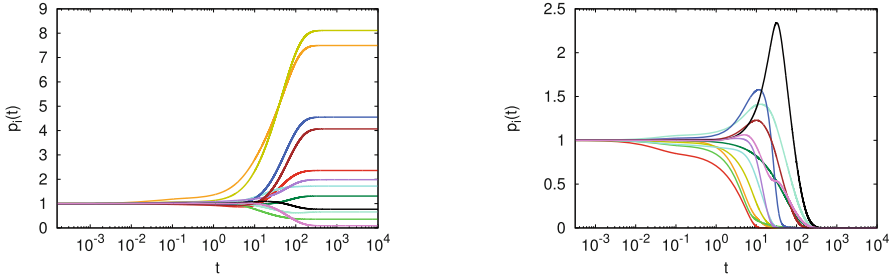


Fig. 2. Time evolution of the densities p_i of the non-monomeric molecules as in Fig. 1, but now with energy consideration, both for the instance displaying an ACM (left) and the instance displaying no ACM (right)

In the next step, we consider the model extended with an energy consideration as introduced in [5]. We use the same instances as before. The computational results are shown in Fig. 2. The instance which displayed an ACM before again shows an ACM, but the resulting values of the densities for the various molecules differ strongly from those in Fig. 1. The other instance again contains no ACM. A further effect of considering the finite available energy is that it retards the dynamics, as the curves for the various molecules start to deviate from the original values significantly later. Furthermore, one can state that the consideration of the energy stabilizes the dynamics, as already mentioned in [5], as the intermediate maxima are much smaller than without energy consideration. The computing time required increases strongly when considering the energy: for the instance with an ACM, the Dornand-Price method requires more than 8.6 million time steps and it takes 8193 time steps for the instance without an ACM.

4.2 Two Separate Containers

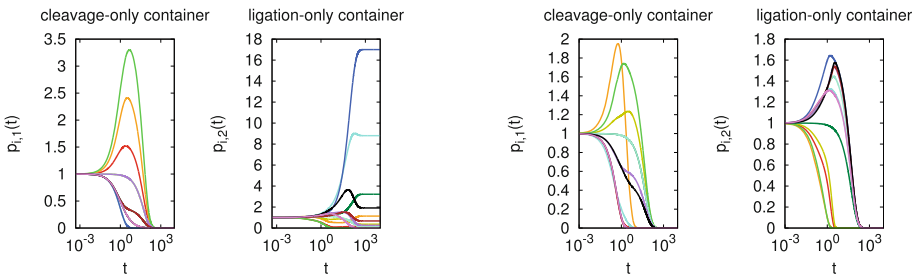


Fig. 3. Time evolution of the densities $p_{i,j}$ of the non-monomeric molecules as in Fig. 1, but now in two separate containers, one of them only allowing cleavage reactions (left part, $j = 1$), the other one only allowing ligation reactions (right part, $j = 2$), both for the instance displaying an ACM (left) and the instance displaying no ACM (right)

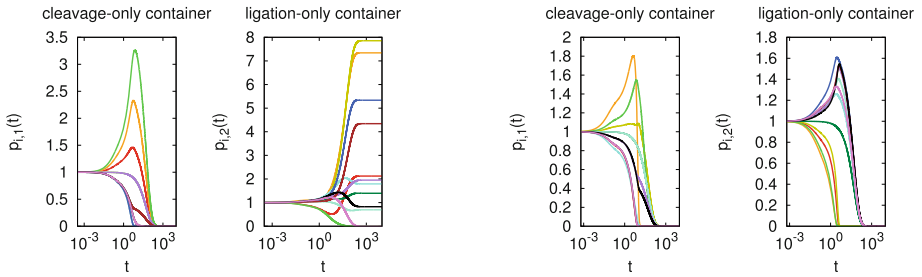


Fig. 4. Time evolution of the densities $p_{i,j}$ of the non-monomeric molecules as in Fig. 3, in two separate containers, one of them only allowing cleavage reactions (left part, $j = 1$), the other one only allowing ligation reactions (right part, $j = 2$), but now with energy consideration, both for the instance displaying an ACM (left) and the instance displaying no ACM (right)

The results discussed so far for one container can also be interpreted as the results obtained with two containers with spatially separated cleavage and ligation reactions if the diffusion takes place so fast that any density differences between the two containers are resolved immediately. Before considering the connected containers with diffusion, we would like to study the other extreme case first, in which the two containers are separate and in which no diffusion takes place. The results for the scenario without considering the energy are shown in Fig. 3, the results for the scenario including the energy in Fig. 4. For the instance, which contained an ACM before, we find that the densities vanish in the container with the cleavage processes as has to be expected (The original densities of the non-monomeric molecules decrease due to outflow and cleavage reactions and no new non-monomeric molecules are formed as there is no ligation. So, there is no ACM.), whereas an ACM can still be found in the container with the ligation processes. We also investigated other instances, for some of them which contained an ACM in one container only there is also no ACM in the container with only ligation processes.

4.3 Two Containers with Diffusion

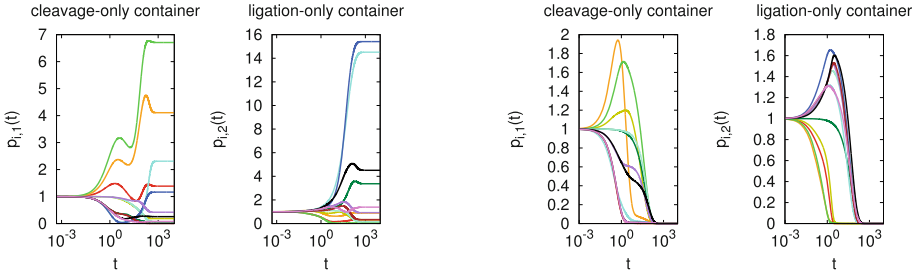


Fig. 5. Time evolution of the densities $p_{i,j}$ of the non-monomeric molecules as in Fig. 3, but now with diffusion between two connected containers, one of them only allowing cleavage reactions (left part, $j = 1$), the other one only allowing ligation reactions (right part, $j = 2$), both for the instance displaying an ACM (left) and the instance displaying no ACM (right)

Finally, we get to the main point of this paper, the Kauffman model implemented with spatially separated cleavage and ligation processes in two containers with diffusion between them. First, we consider diffusion according to formula (10) and present computational results without energy consideration in Fig. 5 and with energy consideration in Fig. 6. We find that the instance which contained an ACM before now contains ACMs in both containers despite the fact that the diffusion constant k_D is set to a very small value. On the other hand, the instance which displayed no ACM before now also shows no ACMs. The molecules whose curves plotted in light blue and light green dominated the ACM in the left picture in Fig. 1 now also belong to the dominating molecules in the ACMs in the left pictures of Fig. 5, but there are now more significant contributions of other molecules as well. The same behavior is found for the molecules plotted in dark yellow and orange when comparing Figs. 2 and 6.

Then we have a look at the diffusion with an increasing number of pores according to formulas (11) and (14). The computational results are shown in Fig. 7 for the scenario without energy consideration and Fig. 8 with consideration of the energy. For the left instance, we again get an ACM, the steps in the curves reflect the opening of an increasing number of pores. These steps are smaller if the energy is considered. As the number of pores increases in time, equilibrium cannot be reached. For the instance without an ACM, we hardly see any steps, the breakdown of the densities dominates the behavior.

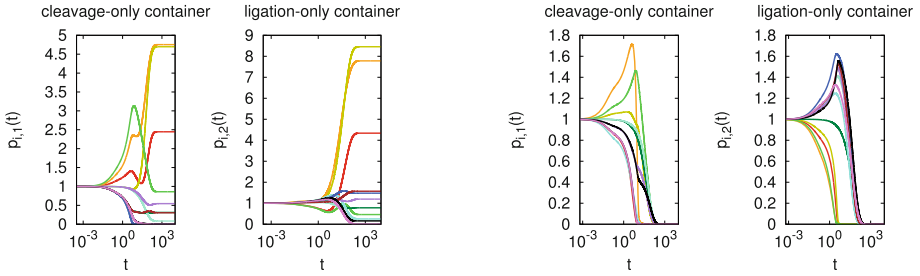


Fig. 6. Time evolution of the densities $p_{i,j}$ of the non-monomeric molecules as in Fig. 5, with diffusion between two connected containers, one of them only allowing cleavage reactions (left part, $j = 1$), the other one only allowing ligation reactions (right part, $j = 2$), but now with energy consideration, both for the instance displaying an ACM (left) and the instance displaying no ACM (right)

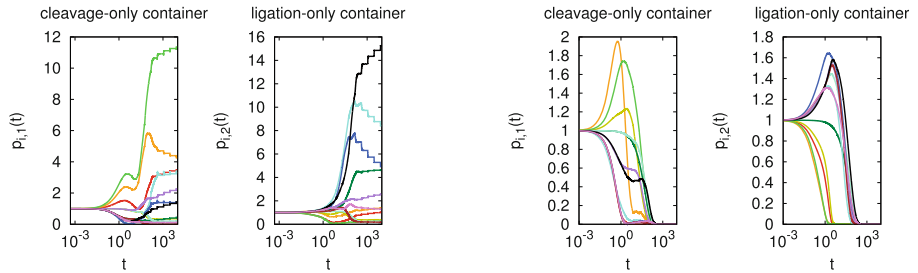


Fig. 7. Time evolution of the densities $p_{i,j}$ of the non-monomeric molecules as in Fig. 5, but now with diffusion through an increasing number of pores between two connected containers, one of them only allowing cleavage reactions (left part, $j = 1$), the other one only allowing ligation reactions (right part, $j = 2$), both for the instance displaying an ACM (left) and the instance displaying no ACM (right)

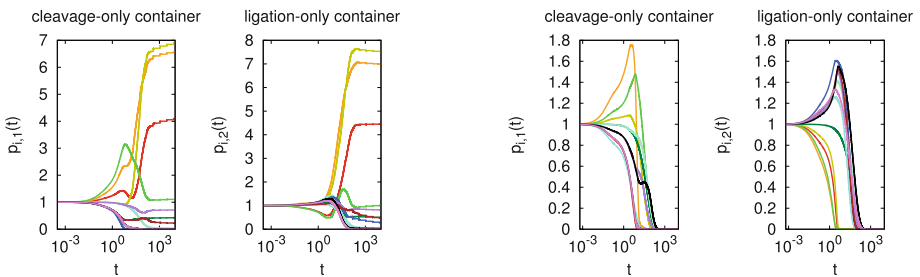


Fig. 8. Time evolution of the densities $p_{i,j}$ of the non-monomeric molecules as in Fig. 7, with diffusion through an increasing number of pores between two connected containers, one of them only allowing cleavage reactions (left part, $j = 1$), the other one only allowing ligation reactions (right part, $j = 2$), but now with energy consideration, both for the instance displaying an ACM (left) and the instance displaying no ACM (right)

4.4 Comparison of Final Dynamics

Finally, we want to get a better insight in the behavior of the Kauffman model and in the roles the various molecules play. For this purpose, we have a close look at the final densities of the various molecules in the instance containing an ACM, for the three scenarios of the original Kauffman model, the model with two separate containers, and the model with two containers connected by diffusion with a time-independent diffusion constant, each without consideration of finite energy. The final values for the densities of the various molecules for these three scenarios are provided in Table 2.

Table 2. Final values for the densities of the various molecules in the instance displaying an ACM for the original Kauffman model, for the extreme case without diffusion, and for the scenario with a constant diffusion constant, without energy consideration

Molecule No. i	original model $p_i(t_{\text{final}})$	no diffusion		with diffusion	
		cleavage-only $p_{i,1}(t_{\text{final}})$	ligation-only $p_{i,2}(t_{\text{final}})$	cleavage-only $p_{i,1}(t_{\text{final}})$	ligation-only $p_{i,2}(t_{\text{final}})$
1	0.505	50	0.457	21.76	0.635
2	0.070	50	6.52E-2	14.71	8.27E-2
3	0.404	2.25E-87	0.155	1.385	0.316
4	0.352	3.64E-87	1.138	4.108	0.889
5	0.145	1.38E-87	0.365	0.184	0.331
6	6.775	5.47E-87	2.47E-323	6.708	6.66E-2
7	0.023	5.08E-88	3.219	4.67E-2	3.369
8	6.15E-5	1.38E-87	0.171	6.80E-2	0.150
9	20.56	2.66E-109	8.803	2.309	14.51
10	1.553	2.66E-109	17.00	1.165	15.41
11	1.416	1.38E-87	0.264	0.420	0.924
12	8.69E-5	5.08E-88	0.677	2.36E-3	0.333
13	2.615	2.71E-89	1.915	0.256	4.511
14	1.856	2.71E-89	2.10E-87	7.91E-2	1.391

Here we first have a look at $p_i(t_{\text{final}})$ for the original model. If choosing a threshold $\geq 10^{-4}$, we could state that the ACM contains all molecules except two. But the question arises whether we are right to exclude molecules Nos. 8 and 12 or whether they play a role in the ACM, even if their final densities are very small. As Table 1 shows, each molecule can be created either by a ligation or by a cleavage reaction or both.

When having a look at the results for the two separate containers, we find as expected that there is no ACM in the cleavage-only container. All longer molecules are destroyed by the cleavage processes and by the outflow. No new longer molecules can be created, as the constant inflow of the two monomers cannot be used for ligation, as there are no ligation reactions. Thus, we get a value of 50 for the densities of the two monomers, which is just the ratio between the inflow and the outflow parameters, and a vanishing value for all other molecules. In the ligation-only container, we get final densities which partially slightly, but

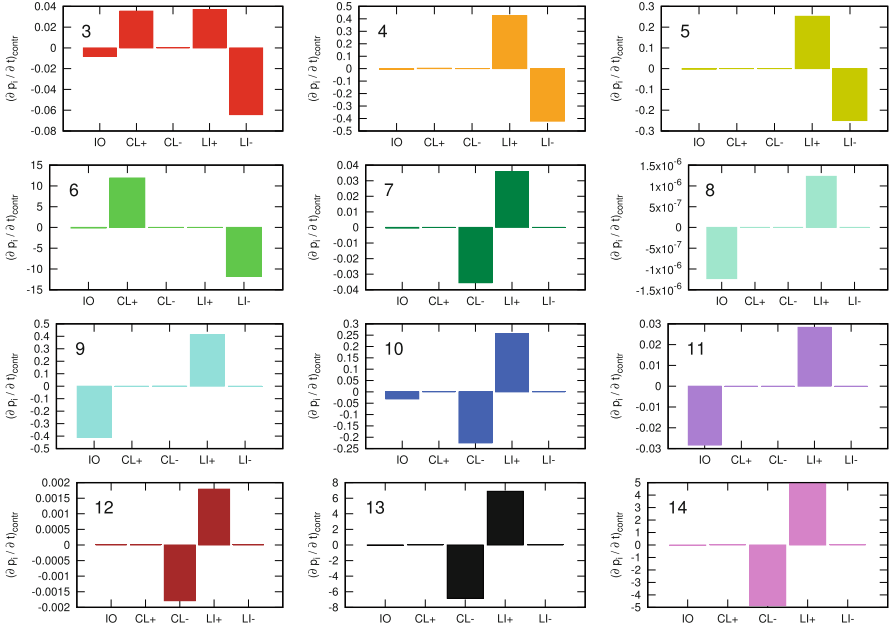


Fig. 9. Final dynamics: final values for the derivatives $(dp_i/dt)_{\text{contr.}}$ of the densities for the various non-monomeric molecules for the instance containing an ACM in the original Kauffman model, for the various contributions: IO – inflow and outflow, CL+ – generated by cleavage processes, CL- – destroyed by cleavage processes, LI+ – generated by ligation processes, LI- – destroyed by ligation processes

most often strongly deviate from the final densities in the original Kauffman scenario. Obviously, the additional cleavage processes in the original Kauffman scenario lead to these large differences. Molecules Nos. 6 and 14 are obviously not part of the ACM anymore, their densities truly vanish.

Then we have a look at the results for two containers connected by diffusion. Here we see that the densities for the molecules Nos. 8 and 12 are much larger in both containers than in the original Kauffman model. Obviously, a spatial separation of reactions can lead to an enlargement of an ACM. But this result also raises questions to the approach of determining the size of an ACM, i.e., the number of molecules being part of an ACM, by excluding those molecules whose densities are smaller than some arbitrarily chosen threshold. Here one has to be very careful of how to choose the value of the threshold, in order to not exclude those molecules which contribute to the ACM, even if their contribution seems to be tiny.

In order to even better understand the final dynamics for these three scenarios, we have a look at the final values for the various contributions to the derivatives of the densities, which are shown for the three scenarios considered here in Figs. 9, 10, and 11. We consider separately the contributions by the

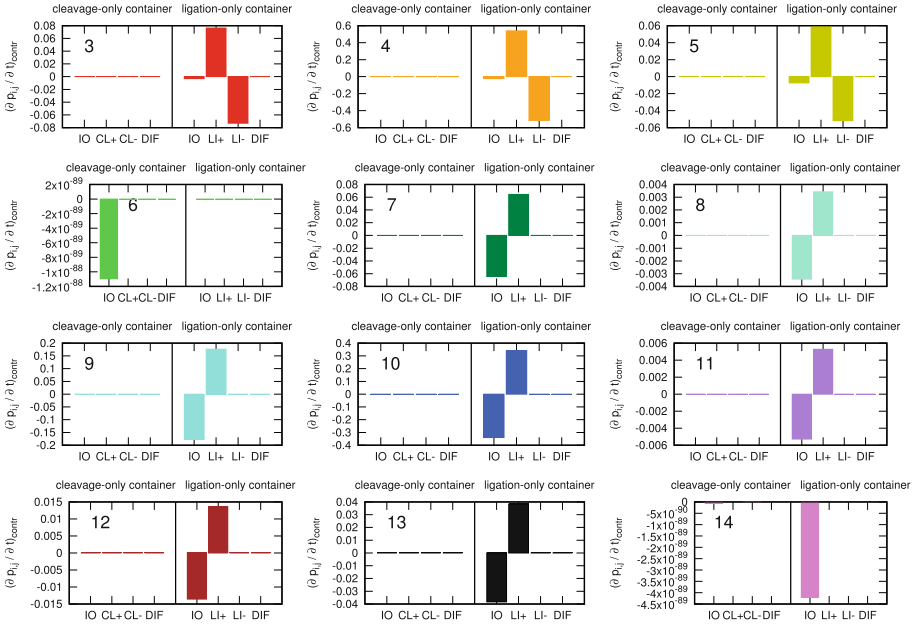


Fig. 10. Final dynamics: final values for the derivatives $(dp_{i,j}/dt)_{\text{contr.}}$ of the densities for the various non-monomeric molecules in the cleavage-only container (left) and the ligation-only container (right) in the scenario with two separate containers, for the various contributions: IO – inflow and outflow, CL+ – generated by cleavage processes, CL- – destroyed by cleavage processes, LI+ – generated by ligation processes, LI- – destroyed by ligation processes, DIF – diffusion

various processes in-out-flow, cleavage, ligation, and diffusion. Already for the original Kauffman model, we see a rich behavior: Molecules 4 and 5 are created by ligation processes but also destroyed by ligation processes, molecules 7, 10, 12, 13, and 14 are created by ligation and destroyed by cleavage, while molecule 6 is created by cleavage and destroyed by ligation. Molecules 8, 9, and 11 are created by ligation, but destroyed by outflow. Molecule 3 exhibits the richest behavior, it is both created by cleavage and ligation and it is destroyed by ligation. Of course, for all of these molecules, also the outflow plays some role, but only for some of them the outflow provides the main contribution to decreasing their densities. Thus, we get a very rich variety of behaviors already here in Fig. 9 for the original Kauffman model. Please note that all the bars in the subgraphs for the various molecules add up to zero, as the final densities are constant such that the sum of all contributions to their derivatives has to vanish.

Figure 10 shows the results for the scenario with two separate containers. As expected, there is no ACM in the cleavage-only container, such that the derivatives vanish there. In the ligation-only container, the derivatives for molecules 6 and 14 vanish as well, they are not part of the ACM here. But all other molecules contribute to the ACM. Molecules 7–13 are created by ligation processes, their

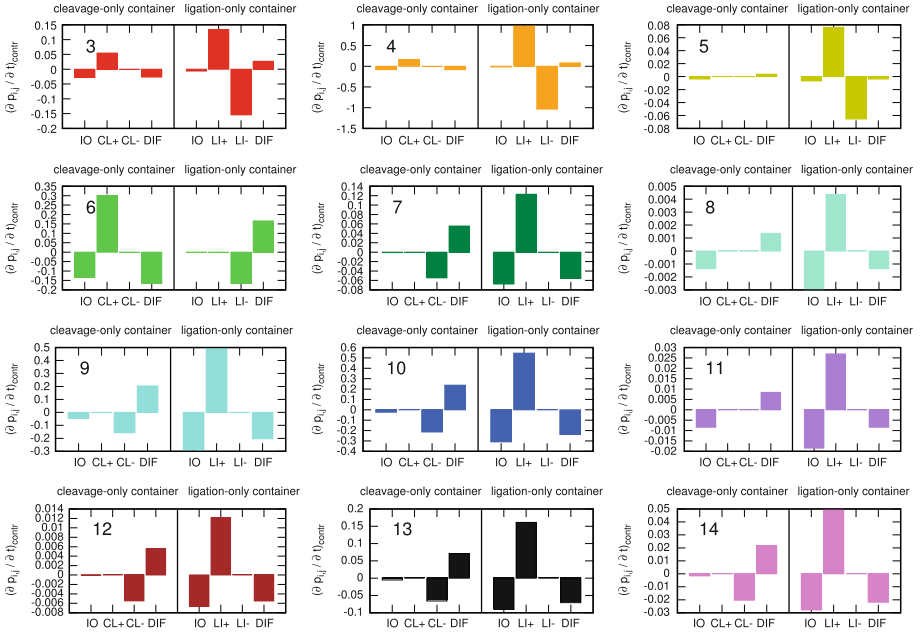


Fig. 11. Final dynamics: final values for the derivatives $(dp_{i,j}/dt)_{\text{contr.}}$ of the densities for the various non-monomeric molecules in the cleavage-only container (left) and the ligation-only container (right) in the scenario with two containers connected by diffusion, for the various contributions: IO – inflow and outflow, CL+ – generated by cleavage processes, CL- – destroyed by cleavage processes, LI+ – generated by ligation processes, LI- – destroyed by ligation processes, DIF – diffusion

densities are reduced by outflow only. Molecules 4 and 5 are both created and destroyed by ligation processes, additionally also outflow is reducing their densities.

Figure 11 shows the corresponding results for the scenario with two containers connected by diffusion, for which we again find interesting behaviors. Molecules 7 and 9–14 share the same behavior: they are produced in the ligation-only container. Part of the density diffuses to the cleavage-only container where the incoming density is destroyed by a cleavage process. In both containers, also the outflow reduces the densities. Like in Fig. 9, molecule 6 demonstrates just the opposite behavior, it is produced by a cleavage process in the cleavage-only container, part of its density diffuses into the ligation-only container, where it is destroyed by a ligation process and the outflow. Molecules 4 and 5 are again dominated by the production and destruction via ligation processes. Please note that also here the bars need to add up to zero, separately for both containers.

5 Conclusion and Outlook

For this paper, we performed simulations for the original Kauffman model, the Kauffman model extended with the consideration of finite energy amounts, and

our approach of spatially separating the cleavage and ligation reactions in two containers connected by diffusion. We present computational results both for a randomly created instance displaying an autocatalytic metabolism (ACM) and for another randomly created instance without an ACM. The densities of the various non-monomeric molecules, which initially start out at the same value, first undergo some intermediate transition. For the instance without the ACM, all of them vanish in the long term in all simulations, whereas in the other instance, the densities of some of the non-monomeric molecules converge to finite values, thus forming the ACM. This other instance continues to display an ACM in all scenarios. While the molecules dominating the ACM in the original Kauffman approach with only one container stay dominant when spatially separating the cleavage from the ligation processes in two different containers, other molecules become dominant when including the energy finiteness. The size of the ACM, i.e., the number of non-monomeric molecules with significant final density values, increases when spatially separating cleavage from ligation processes. Studying the final values for the contributions of the various processes to the derivatives of the probabilities, we get a rich behavior, with some molecules produced and destroyed by ligation processes, others produced by ligation and destroyed by cleavage processes, and one molecule produced by cleavage and destroyed by ligation processes. These results are to be expected, they reflect the list of reactions in Table 1. This close look at the contributions to the overall derivative obviously provides a better insight whether a molecule is part of the ACM than the comparison of its density to an arbitrarily chosen threshold.

We intend to continue our investigations by creating larger statistics of these scenarios and by applying all of them to large networks of spatially connected droplets [15–19], in which either only ligation or only cleavage reactions are performed. Depending on the simulation parameters, we expect to be able to enlarge the probability for the occurrence of an ACM, for those instances in which it is possible from a graph-theoretical aspect, but in which the dynamics prevents the creation of an ACM in one container only. We also expect to get much larger average sizes of an ACM. These large networks also provide a further advantage: While it is impossible to change the kinetic parameters for the reactions as well as the diffusion and transport parameters for real systems, large networks of droplets with spatially separated reactions allow to put more emphasis on some reactions, e.g., to implement many more droplets with ligation than with cleavage reactions, thus increasing the probability for the occurrence of an ACM.

Furthermore, instead of using the approach to set up and numerically solve a set of differential equations, we alternatively intend to apply a stochastic simulation framework, e.g., to work with the Gillespie algorithm [2, 6], which we recently applied to a minimum reaction system with one undesired side product [20]. The Gillespie algorithm is better suited for large numbers of small containers in which the number of the various molecules could be so small that the continuous density approach is no longer justified. This stochastic simulation framework offers new possibilities and new insights, but also leads to further difficulties: Here we would not have to depend on the value of a threshold for a

density whether we would consider a specific molecule to be part of the ACM or not. When using the Gillespie algorithm with its integer numbers for various molecules, we can simply state that a molecule is not part of the ACM if its number is exactly zero over a sufficiently long time period. However, in another simulation run, it might be the case that this molecule does not vanish and thus is part of the ACM. Thus, the shape of the ACM achieved with the Gillespie algorithm might depend on whether some number of catalyst molecules necessary for some reactions become exactly zero due to a specific sequence of stochastic random choices of reactions or due to the late opening up of pores, or due to some other reasons, whereas in the continuous density approach, the density might become very small but then has the chance to increase again.

References

1. Bagley, R., Farmer, J.: Spontaneous emergence of a metabolism. In: Langton, C., Taylor, C., Farmer, J., Rasmussen, S. (eds.) *Artificial Life II*, Santa Fe Institute Studies in the Sciences of Complexity, vol. X, pp. 93–140. Addison-Wesley, Redwood City (1991)
2. Cieslak, M., Prusinkiewicz, P.: Gillespie-lindenmayer systems for stochastic simulation of morphogenesis. in *silico Plants* **1**, diz009 (2019)
3. Dormand, J.R., Prince, P.J.: A family of embedded Runge-Kutta formulae. *J. Comput. Appl. Math.* **6**(1), 19–26 (1980)
4. Fick, A.: Ueber diffusion. *Ann. Phys.* **170**(1), 59–86 (1855). <https://doi.org/10.1002/andp.18551700105>
5. Füchslin, R.M., Filisetti, A., Serra, R., Villani, M., Lucrezia, D.D., Poli, I.: Dynamical stability of autocatalytic sets. In: Fellermann, H., et al. (eds.) *Proceedings of the Twelfth International Conference on the Synthesis and Simulation of Living Systems, ALIFE 2010*, Odense, Denmark, 19–23 August 2010, pp. 65–72. MIT Press (2010). https://digitalcollection.zhaw.ch/bitstream/11475/2722/1/2010_Fuechslin_Dynamical%20stability%20of%20autocatalytic%20sets_Artificial%20live%20XII.pdf
6. Gillespie, D.T.: A general method for numerically simulating the stochastic time evolution of coupled chemical reactions. *J. Comput. Phys.* **22**, 403–434 (1976)
7. Hordijk, W.: A history of autocatalytic sets: a tribute to Stuart Kauffman. *Biol. Theory* **14**, 224–246 (2019)
8. Hordijk, W., Steel, M.: Detecting autocatalytic, self-sustaining sets in chemical reaction systems. *J. Theor. Biol.* **227**, 451–461 (2004)
9. Hordijk, W., Steel, M., Kauffman, S.: Autocatalytic sets arising in a combinatorial model of chemical evolution. *Life* **12**(11), 1703 (2022)
10. Kauffman, S., Steel, M.: The expected number of viable autocatalytic sets in chemical reaction systems. *Artif. Life* **27**(1), 1–14 (2021)
11. Kauffman, S.A.: Cellular homeostasis, epigenesis and replication in randomly aggregated macromolecular systems. *J. Cybern.* **1**(1), 71–96 (1971)
12. Kauffman, S.A.: Autocatalytic sets of proteins. *J. Theor. Biol.* **119**(1), 1–24 (1986)
13. Kauffman, S.A.: *The Origins of Order: Self-Organization and Selection in Evolution*. Oxford University Press, New York (1993)
14. Oparin, A.: *The Origin of Life on the Earth*, 3rd edn. Academic Press, New York (1957)

15. Schneider, J.J., Weyland, M.S., Flumini, D., Füchslin, R.M.: Investigating three-dimensional arrangements of droplets. In: Cicirelli, F., Guerrieri, A., Pizzuti, C., Socievole, A., Spezzano, G., Vinci, A. (eds.) WIVACE 2019. CCIS, vol. 1200, pp. 171–184. Springer, Cham (2020). https://doi.org/10.1007/978-3-030-45016-8_17
16. Schneider, J.J., Weyland, M.S., Flumini, D., Matuttis, H.-G., Morgenstern, I., Füchslin, R.M.: Studying and simulating the three-dimensional arrangement of droplets. In: Cicirelli, F., Guerrieri, A., Pizzuti, C., Socievole, A., Spezzano, G., Vinci, A. (eds.) WIVACE 2019. CCIS, vol. 1200, pp. 158–170. Springer, Cham (2020). https://doi.org/10.1007/978-3-030-45016-8_16
17. Schneider, J.J., et al.: Network creation during agglomeration processes of polydisperse and monodisperse systems of droplets. In: De Stefano, C., Fontanella, F., Vanneschi, L. (eds.) WIVACE 2022. CCIS, vol. 1780, pp. 94–106. Springer, Cham (2023). https://doi.org/10.1007/978-3-031-31183-3_8
18. Schneider, J.J., et al.: Influence of the geometry on the agglomeration of a polydisperse binary system of spherical particles. In: ALIFE 2021: The 2021 Conference on Artificial Life (2021). <https://doi.org/10.1162/isal.a.00392>
19. Schneider, J.J., et al.: Paths in a network of polydisperse spherical droplets. In: ALIFE 2022: The 2022 Conference on Artificial Life (2022). <https://doi.org/10.1162/isal.a.00502>
20. Schneider, J.J., et al.: Artificial chemistry performed in agglomeration of droplets with restricted molecule transfer. In: De Stefano, C., Fontanella, F., Vanneschi, L. (eds.) WIVACE 2022. CCIS, vol. 1780, pp. 107–118. Springer, Cham (2023). https://doi.org/10.1007/978-3-031-31183-3_9
21. Xavier, J.C., Kauffman, S.A.: Small-molecule autocatalytic networks are universal metabolic fossils. *Phil. Trans. R. Soc. A* **380**, 20210244 (2022)

Open Access This chapter is licensed under the terms of the Creative Commons Attribution 4.0 International License (<http://creativecommons.org/licenses/by/4.0/>), which permits use, sharing, adaptation, distribution and reproduction in any medium or format, as long as you give appropriate credit to the original author(s) and the source, provide a link to the Creative Commons license and indicate if changes were made.

The images or other third party material in this chapter are included in the chapter's Creative Commons license, unless indicated otherwise in a credit line to the material. If material is not included in the chapter's Creative Commons license and your intended use is not permitted by statutory regulation or exceeds the permitted use, you will need to obtain permission directly from the copyright holder.

